

In-Band Label Extractor Based on Cascaded Si Ring Resonators Enabling 160Gb/s Optical Packet Switching Modules

Peter De Heyn, *Student Member, IEEE*, Jun Luo, *Member, IEEE*, Stefano Di Lucente *Student Member, IEEE*, Nicola Calabretta, *Member, IEEE*, Harm J. S. Dorren, *Member, IEEE*, Dries Van Thourhout, *Member, IEEE*

Abstract—Photonic integration of optical packet switching modules is crucial to compete with existing electronic switching fabrics in large data center networks. The approach of coding the forwarding packet information in an in-band label enables a spectral-efficient and scalable way of building low-latency large port count modular optical packet switching architecture. We demonstrate the error-free operation of the four in-band label extraction from 160 Gb/s optical data packets based on photonic integrated silicon-on-insulator ring resonators. Four low-loss cascaded ring resonators using the quasi-TM mode are used as narrowband filters to ensure the detection of four optical labels as well as the error-free forwarding of the payload at limited power penalty. Due to the low-loss and less-confined optical quasi-TM mode the resonators can be very narrowband and have low insertion loss. The effect of the bandwidth of the four ring resonators on the quality of the payload is investigated. We show that using four rings with 3dB bandwidth of 21 pm and only an insertion loss of 3 dB, the distortion on the payload is limited (< 1.5 dB power penalty), even when the resonances are placed very close to the packet's central wavelength. We also investigate the optical power requirements for error-free detection of the label as function of their spectral position relative to the center of the payload. The successful in-band positioning of the labels makes this component very scalable in amount of labels.

Index Terms—Silicon-on-Insulator, Ring Resonators, Optical Packet Switch, Optical Label Processor.

I. INTRODUCTION

The ever increasing demand on the performance of large data center networks and supercomputers computing at tens of petaflops per second is creating a communication bottle neck among the thousands of nodes within these systems [1], [2]. Especially the port-count dependent latency and the many power hungry optical-to-electrical and electrical-to-optical conversions of current electronic switches have limited the scalability of these systems [3]. This has motivated research on low latency and large port-count optical packet switches (OPS).

Packets entering these OPS are labeled with forwarding information to properly configure the switch and set the packet destination. Several techniques have been investigated so far

to enable a fast, low cost, and low power label processing. A typical scheme consists of serial time multiplexing the optical label at the head of the packets on the same wavelength [4]. In order to prevent any degradation of the payload during the label erasure and insertion, this approach requires guard times in between the label and the payload. A drawback of serial time multiplexing the label is that it requires time consuming bit synchronization and clock recovery circuits that introduce large latency. To address the large guard times, approaches making use of parallel label bit processing have been proposed [5]–[8]. This allows for an asynchronous label bit processing but is still limited in label recognition times as discussed in [9], independent of the coding technique being used. To reduce the latency further, the parallel encode label is wavelength division multiplexed (WDM) and hence the label can be processed in parallel allowing for shorter latency times. A novel modular WDM optical packet switch architecture using parallel multiplexed coding together with an in-band optical label technique has been proposed and demonstrated both numerically and experimentally [9], [10].

In this architecture (shown in Fig.1) each module forwards an arbitrary number (M) of WDM packets to an arbitrary number (N) of output ports, based on the information encoded in the optical label. The optical label, which can consist of different optical frequency components, is transmitted in-band with the optical payload to maximize the optical spectral efficiency and to allow an asynchronous and hence more straightforward extraction of the label. If the available optical bandwidth is too limited one can easily increase the number of addresses through the use of RF tone coding [11]. Several techniques for label extraction of in-band labeling based on discrete components have been previously demonstrated [6], [12].

To drastically decrease the size, unit cost and power consumption of the proposed OPS and to be able to compete with power efficient and mass-manufacturable electronic switches integration of the different optical building blocks is absolutely necessary. In [9] an optical packet switch built using integrated InP 1×4 optical wavelength-space switching modules was shown to exhibit a reduced power consumption but still used a discrete and bulky optical label processor. Enabling the proposed spectrally-efficient in-band labeling requires narrowband drop filters to extract the low-speed labels from a high-speed payload. This filter could e.g. be an integrated ring resonator as was demonstrated in [13] were signals at

P. De Heyn, D. Van Thourhout are with the Photonics Research Group, Department of Information Technology, Ghent University - imec, B-9000 Ghent, Belgium (email:peter.deheyn@intec.ugent.be)

Jun Luo, Stefano Di Lucente, Nicola Calabretta and Harm Dorren are with Department of Electrical Engineering, Technical University of Eindhoven (TU/e), 5600MB Eindhoven, The Netherlands

Manuscript received...; revised ...

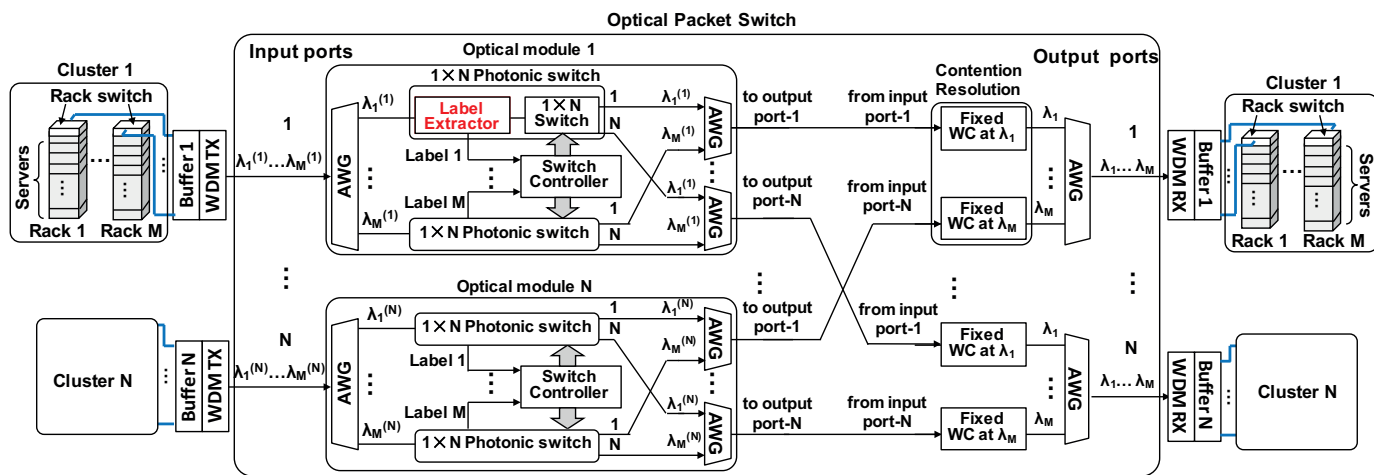


Fig. 1. Example of a modular WDM optical packet switch architecture, demonstrated both numerically and experimentally in [9], [10].

160 Gb/s were successfully switched. In that demonstration a single Si_3N_4 ring resonator ring followed by an external arrayed waveguide grating was used to extract two in-band labels.

In the current work we demonstrate a label extractor consisting of our cascaded narrowband ring resonators implemented in a low loss silicon-on-insulator (SOI) waveguide platform. A higher-index contrast system such as SOI confines the light more strongly and hence allows smaller bending radii. This allows fabricating narrowband filters with larger free spectral ranges (FSR). It also permits a higher integration density compared to lower-index contrast systems such as those based on InP or SiN based systems which is essential when scaling to larger port numbers.

Our ring resonators are using the low-loss and less-confined quasi-TM mode. The quasi-TM mode is used to create resonances with a bandwidth (BW) as narrow as 17 pm. Using this label extractor we demonstrate the successful extraction of four in-band labels and error free operation of the 160 Gb/s payload. The performance of the ring regarding insertion loss, extinction ratio and BW (ultimately limited by its loss) is shown to have a large influence on the quality of the extracted label and forwarded payload and a trade-off between different devices and parameters is studied. The minimum required label power relative to the payload to reach a certain bit-error rate is also investigated. We found that this power depends on the spectral position of the label with respect to the center of the payload.

The design and fabrication of the SOI integrated device are discussed in section II. Section III presents the experimental results, starting with the characterization of the ring resonator in III-A, whereby we focus on the trade-off between different performance specifications. In section III-B the experimental setup is briefly introduced and in section III-C the full system characterization, including comprehensive bit-error rate measurements of the forwarded payload as well of the extracted labels are reported.

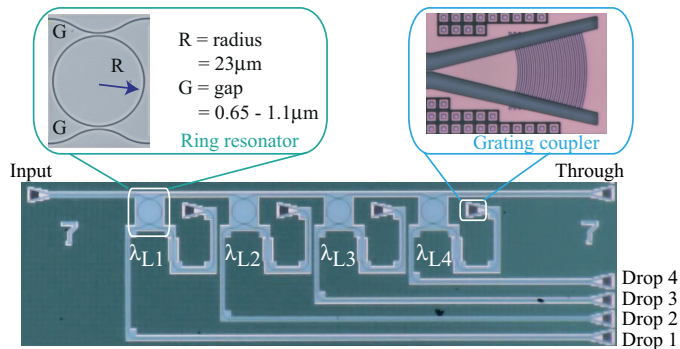


Fig. 2. Microscopic picture of the label extractor based on four narrowband Si ring resonators using the quasi-TM mode. The device has one input and five outputs. The through port contains the payload without labels and the four drop ports contain one extracted label.

II. FABRICATION AND DESIGN

A. Fabrication

The four-channel label extractor was fabricated on a 200 mm SOI wafer with 2 μm buried oxide and 220 nm top c-Si layer. Two silicon patterning steps were carried out in which respectively 70 nm and 220 nm of the c-Si layer were locally etched to define fiber-grating couplers as well as the ring filter and the access waveguides. A microscopic picture of the fabricated device is shown in Fig.2.

B. Design

A well-known drawback of highly confined standard single-mode silicon waveguides (450 nm wide x 220 nm high) is the sensitivity to vertical sidewall roughness on the quasi-TE mode. This typically causes wavelength depending backscattering, which can add up coherently in high-quality (Q) factor filters and will consequently result in filters with an unacceptable high and wavelength depending insertion loss and resonance splitting [14]. Several options exist to lower the field overlap with the vertical sidewall roughness. A first option is to use the quasi-TM mode in fully etched strip waveguide. This mode is less confined than the TE-like mode and has been

used to demonstrate ring resonators exhibiting an improved Q-factor without resonance splitting [14]. An alternative is to use the quasi-TE mode in a partially etched rib waveguide. Also this approach allows to lower the overlap with vertical sidewall roughness and has been proven to enable high-Q all-pass filters [15]. In both cases the waveguide confinement decreases, requiring somewhat higher bend radii and hence limiting the free spectral range to 4 – 5 nm.

In this paper we will focus on the use of the quasi-TM mode to optimize the ring parameters. Fiber-grating couplers designed for the quasi-TM mode are used to couple the light on chip, as shown in the right inset of Fig.2. The waveguides have a height of 220 nm and a width of 500 nm. In designing the first-order ring resonator, the free spectral range was set to 5 nm, which is approximately the 20 dB bandwidth of the 160 Gb/s payload resulting in a radius of 23 μm . We used the analytical description of the spectral behavior of ring resonators as described in [16].

To explore the effect of the bandwidth of the ring resonator, the gap between the bus and ring waveguide was swept between 0.65 μm and 1.1 μm . This gap range is estimated based on the coupling strength between the bus and ring waveguide calculated with a 2D mode solver (Photon Design). All four rings were designed equally but due to some local non-uniformity the resonances of the ring resonator are not overlapping. The quasi-TM mode is particularly sensitive to height deviations of the silicon waveguide due to its tight vertical confinement of the electrical field. In a later step, heaters can be integrated to tune the resonances on the desired grid or spectral position [17].

III. EXPERIMENTAL RESULTS

We start this section with the characterization of the ring resonator and discussing how the different filter specifications change in function of the bus-to-ring waveguide coupling. Then, using the optimized ring resonators, we demonstrate the extraction of four in-band labels from a 160 Gb/s payload.

A. Characterization of the ring resonator

The label extractor was characterized using a tunable laser with a resolution of 1 pm centered around 1550 nm. Fig.3 shows how the main characteristics of the label filter vary as function of the bus-to-ring waveguide gap, with (a) the insertion loss (IL), (b) the extinction ratio (ER) defined by the drop power at resonance with respect to off resonance, (c) the 3 dB BW and (d) the Q-factor.

These results show there is a trade-off between efficiency of the label extraction and power penalties induced on the forwarded payload. To minimize the power penalty on the payload the ring resonators with the smallest bandwidth are preferred since these will erase the smallest amount of signal power of the payload. In Fig.4, the effect of the resonance bandwidth on the payload is investigated. The BER of the payload with a fixed input power versus the Q-factor of the four rings is plotted. The full setup is explained in the following section (section III-C). Note that no labels were added to the payload in this case. The resonance wavelengths

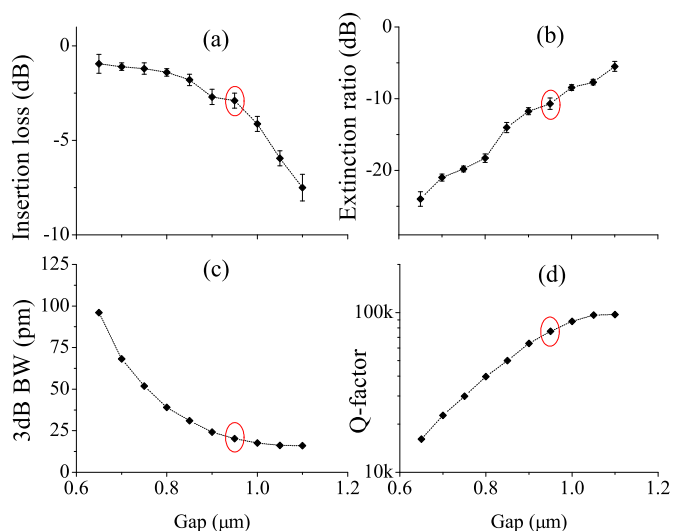


Fig. 3. Overview of the main characteristics of the ring resonators, with (a) the insertion loss, (b) the extinction ratio, (c) the 3dB bandwidth (BW) and (d) the Q-factor, all as function of the gap width. For a larger gap, the insertion loss and Q-factor increase, while the extinction ratio and bandwidth decrease. The performance parameters for the chosen device with gap 0.95 μm are denoted with a circle.

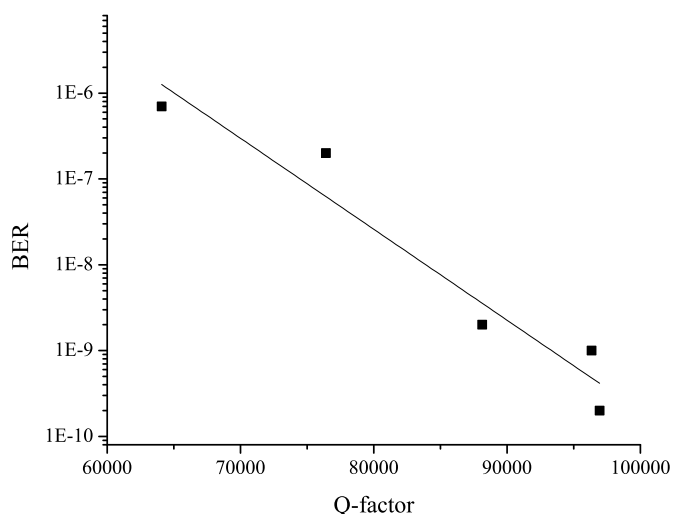


Fig. 4. The relationship between the BER of the payload and the bandwidth (Q-factor) of the four label extractors. The power of the payload is kept constant and received as -9 dBm. The larger the Q-factor, the less signal power of the payload is erased and thus the better the BER.

of the ring resonators are different for each device. However, all of resonances are within the fundamental and the second 160 Gb/s harmonic of payload and none of the resonances is overlapping with each other. One can see that the BER of the payload is indeed improving drastically for increasing Q-factor as expected, which is the result of both a smaller ER and a more narrow BW for the higher Q-factor devices.

Another positive effect of using ring filters with a smaller bandwidth is the decreasing fraction of the payload that is found in the dropped label, resulting in an improved optical signal to noise ratio for constant label and payload input power.

However, at the same time the IL becomes larger (Fig.3a) exceeding 5 dB for a gap ≥ 1.05 μm . This can be understood

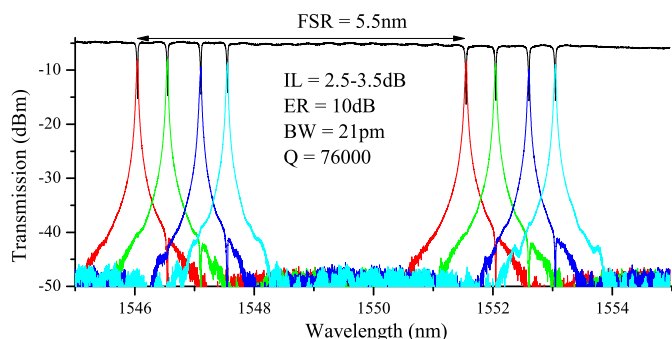


Fig. 5. Filter characterization of the 4-channel label extractor based on narrowband ring resonators using the quasi-TM mode.

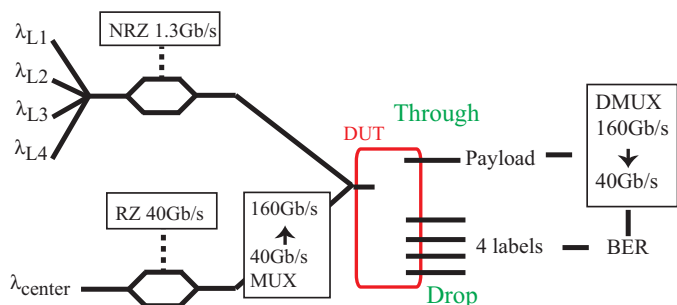


Fig. 6. The setup consisting of label and payload creation, coupled together into the DUT. After label extraction the payload is demultiplexed to 40 Gb/s for BER measurements.

from the fact that the light is longer in the ring before it can exit the ring and therefore exhibits more attenuation due to waveguide losses. For the same reason also the ER is smaller for narrow-band ring resonators. This results in more power of the label remaining in the payload and thus potentially lowers the quality of the payload.

Based on these figures of merit, we choose to use the device with ring resonators with gap of $0.95 \mu\text{m}$ to perform a system test. The spectral characteristics of this label extractor are shown in Fig.5. The FSR is 5.5 nm, the IL is between 2.5 – 3.5 dB depending on the channel and the ER is 10 dB. The non uniformity between the channels IL and ER is most likely coming from small deviations in waveguide losses. The quality factor (Q) of each ring resonator is around 76000, corresponding with a 3 dB BW of 21 pm.

B. System test

The experimental setup employed is shown in Fig.6, where also the location of the through and drop ports is indicated. The small bandwidth of the filters requires a stable temperature which is ensured by a temperature-controlled chip stage. The spectrum of the label extractor input signal consisting of a 160 Gb/s modulated payload and four labels modulated at 1.3 Gb/s is shown in Fig.7(a). The payload is generated by time-quadrupling a 40 Gb/s data stream consisting of 256 return-to-zero bits into a 160 Gb/s data stream using a passive pulse interleaver. Note that in this way the generation of the 160 Gb/s signal is not phase coherent, and the interference

between the adjacent bits will therefore cause a variation of the various harmonics clearly visible when comparing the different spectra shown in Fig.7. In order to obtain a phase coherent signal, the OTDM 160 Gb/s signal may be wavelength converted before adding the labels to the signal [18]. The 1.4 ps optical pulses make the -20 dB bandwidth of the payload to be 5 nm. The center wavelength of the payload is 1552.2 nm and has a total input power of 3.7 dBm.

The four labels are generated with four tunable continuous-wave lasers and are placed exactly on the resonances of the ring filters, with wavelengths as denoted in Fig.7(a). The power of each label is set to -8.9 dBm making the total label power equal to -2.9 dBm. At this power level, the payload after label extraction is error free (error rate = 10^{-9}). The output spectra measured at the drop ports of the ring filters are plotted in Fig.7(b). The location of the ports is shown in Fig.2. Each label signal has an amount of noise coming from the payload signal. One can see that the amount of noise is larger for label 4 than for label 1. This is understood by the relative spectral distance of the labels with payload's center wavelength (defined as the largest frequency component). For label 4 this distance is indeed much smaller than for label 1, respectively located at 0.4 nm and 1.9 nm away from the payload's center wavelength. One can also see a smaller amount of noise at shorter wavelengths coming from the adjacent resonances of the ring filters. The output spectrum after label extraction, measured at the through port of the cascaded ring filters, is shown in Fig.7(c). Each label is dropped by ≈ 10 dB with respect to the payload, which corresponds to the ER of the ring resonator plotted in Fig.3. The total output power of the payload is -9.2 dBm at the through port of our device, showing a total IL of 12.9 dB. We can contribute most of the loss to the grating couplers.

The quality of the payload after label extraction is assessed through a bit-error rate measurement of the four demultiplexed 40 Gb/s signals and is compared with the case where the payload without labels is sent directly to the receiver (denoted as back-to-back). The results are shown in Fig.8. One can see that the power penalty introduced by the label extractor is < 1.5 dB. This power penalty partly results from the fact that some signal power of the payload is filtered out when passing through the label extractor and partly from the four labels which are not perfectly removed and therefore are adding an extra noise floor to the payload. We want to highlight that the BER measurements for the payload in Fig.8 are collected by using a receiver with different sensitivity with respect to the one employed in Fig.4.

The quality of the four in-band labels after extraction from the payload is evaluated as well and compared to the input condition of the label, denoted as back-to-back in Fig.9. To provide more insight, only the power of the label is changed while keeping the power of the payload constant. Since the signal bandwidth of the label modulated at 1.3 Gb/s is small (3 dB BW of 7.2 pm), no distortion is expected from the ring resonator with a 3 dB BW of 21 pm. In other words, the optical lifetime of the signal in the ring is short enough to not affect the signal quality of the label. The only noise is coming from the fraction of the payload passing through to the drop port.

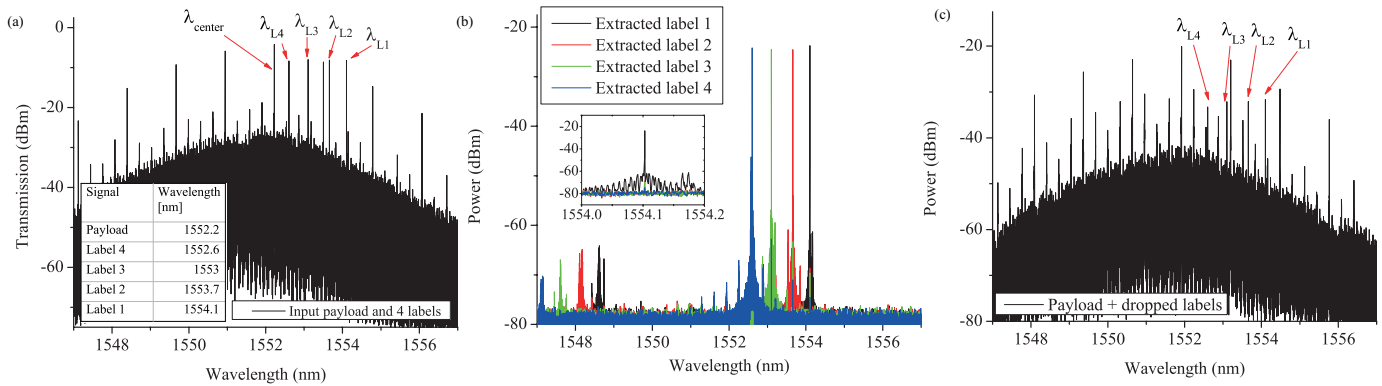


Fig. 7. Optical spectra from the input and outputs with in (a) the input spectrum of the label extractor consisting of a 160 Gb/s modulated payload signal centered at 1552.2 nm and four 1.3 Gb/s modulated label signals and the output spectra of (b) the four labels measured at the drop port and (c) the through port of the label extractor. The location of each port is shown in Fig.2.

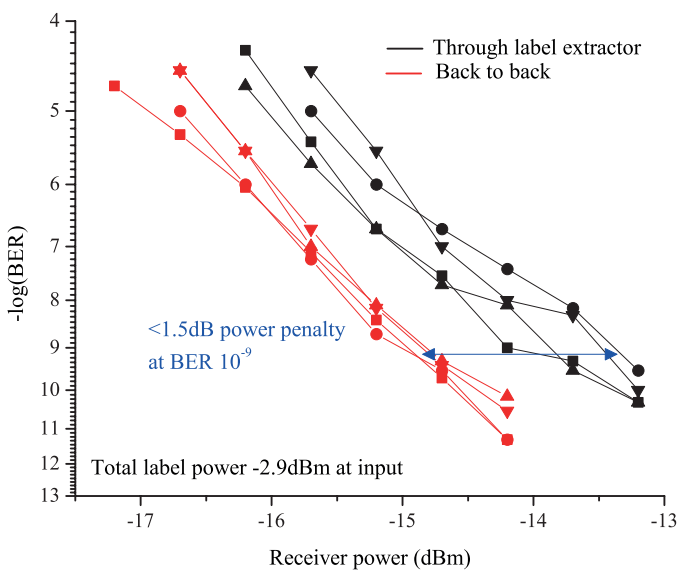


Fig. 8. Bit-error rate measurements of the payload after label extraction. The power penalty introduced compared with the payload without labels before the device (denoted as back-to-back) is less than 1.5 dB.

Increasing the power of the payload therefore decreases the optical signal-to-noise ratio (OSNR) and thus the bit error rate (BER). This ratio is defined by the amount of label power divided by the payload power both measured separately at a certain drop port of the label extractor and is denoted explicitly for each data point in Fig.9. The difference in spectral position with respect to the center wavelength of the payload has a clear impact on the power penalty of the different labels. Label 1, which is further away payload's center wavelength, only has a power penalty of approximately 1 dB while label 4, which is near the center of the payload, has the largest power penalty of 4 dB. One can also see that an OSNR close to 11 is a necessary condition to achieve error-free (EF) operation of the label (i.e. error rate = 10^{-9}), independent from the spectral position of the label. An exception is label 4, where the OSNR required for EF operation is only 9.5, which is probably due to the fact that this label is very close to payload's center wavelength.

The relationship between the BER and the OSNR is plotted

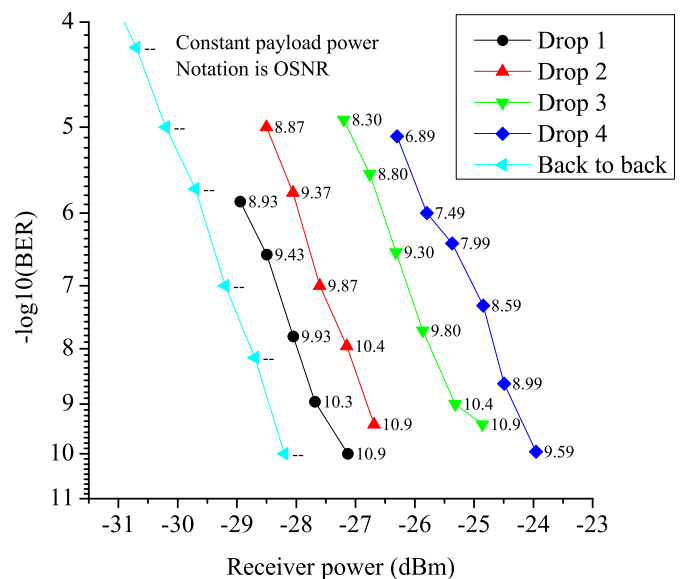


Fig. 9. Bit-error rate measurements of the four labels compared with the input condition of the label (back-to-back). The power of the payload is kept constant to provide more insight based on the optical signal-to-noise ratio (OSNR). Label 1 has a smaller power penalty than label 4 due to its spectral position further away from the payload's center wavelength.

in a different way in Fig.10, where one can indeed see that label 1, 2 and 3 are following the same trend while label 4 is shifted. The power of each label can now be adjusted depending on the spectral distance away from the payload's center wavelength and on the required BER. The spectra of the EF received labels are plotted in Fig.11 with input powers of -10.1 dB, -9.6 dBm, -7.4 dBm and -5.9 dBm for respectively label 1, 2, 3 and 4. This brings the total power of the 4-channel label to -1.89 dBm which is 1 dB more than the total label power used initially to assess the quality of the payload. Fig.11 also shows the eye diagrams of the four different labels at EF operation, plotted on the same scale, where label 4 has indeed the largest noise level.

If the system requires smaller label input powers, e.g. due to power limitations, one can shift the resonances with respect to the payload and work at lower power penalties for the labels.

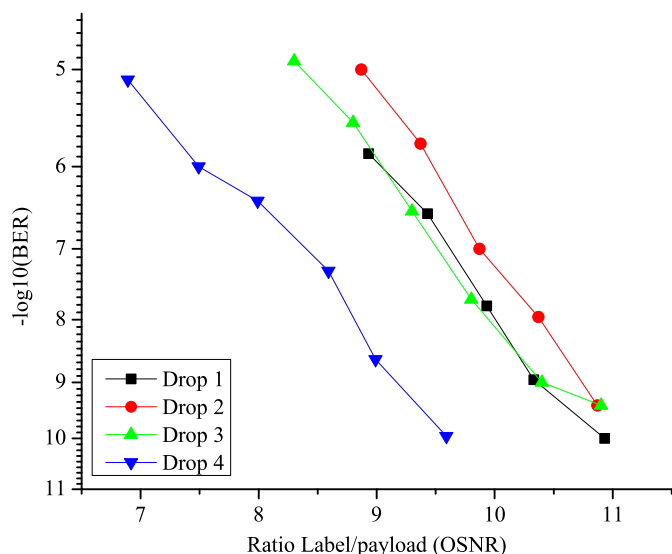


Fig. 10. The bit-error rate versus the optical signal-to-noise ratio (OSNR) for the different labels, each for different payload and label power. Label 1, 2 and 3 are following a similar trend, where as label 4 has a slightly different trend due to close spectral distance to the center of the payload.

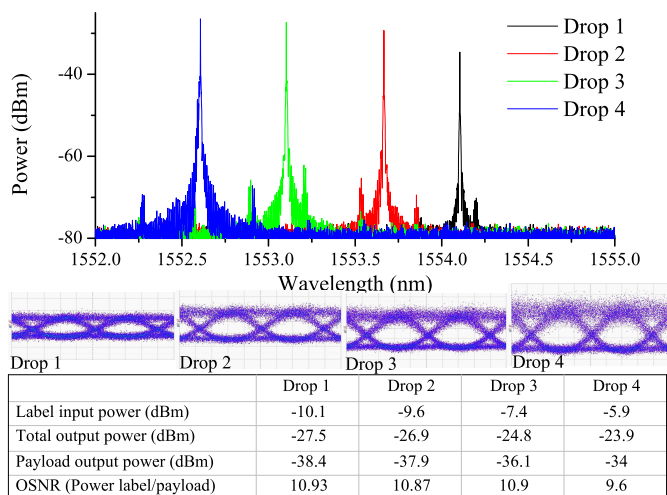


Fig. 11. The spectra of the four received labels at error free ($BER = 10^{-9}$) condition. The signal power of the different labels before and after the chip are denoted in the table, as well as the received amount of payload per label channel and the resulting optical signal-to-noise ratio (OSNR).

IV. CONCLUSION

In this paper an in-band label extractor based on narrow-bandwidth silicon ring resonators using the low-loss quasi-TM mode is investigated. A trade-off between different ring resonator designs regarding relevant filter specifications such as insertion loss, extinction ratio and bandwidth is made. The selected device consisting of four cascaded ring filters with an insertion loss of 3 dB, and extinction ratio of 10 dB and a bandwidth of 21 pm, was shown to be able to extract four in-band labels modulated at 1.3 Gb/s from a 160 Gb/s payload. The quality of the payload as well as the quality of the four labels was evaluated showing error free operation at < 1.5 dB power penalty for the payload. The power penalty of the label depends on the exact spectral position with respect to the

center of the payload and ranges between 1 dB and 4 dB in our study. It has been shown before that filter position can be tuned using integrated heaters [17]. This gives the designer the freedom to optimize the exact spectral position of the labels based on system requirements regarding bit-error rate, power limitations, amount of labels etc. Positioning extra labels further away from the payload's center wavelength will not add extra distortion to the payload and lower label powers can be used. The amount of labels can then further be multiplied by using several RF tones [10] making this label approach flexible and scalable in terms of amount of labels. In a next step highly responsive photodiodes can be integrated directly with the label extractor as we showed before [17]. This will result in a more efficient OE conversion of the label because there is no off-chip insertion loss.

ACKNOWLEDGEMENT

This work is supported by the ERC project ULPPIC and the LIGHTNESS project.

REFERENCES

- [1] C. Kachris and I. Tomkos, "A Survey on Optical Interconnects for Data Centers," *IEEE Communications Surveys & Tutorials*, vol. 14, no. 4, pp. 1021–1036, 2012.
- [2] European Union's 7th Framework Programme, "LIGHTNESS: Low latency and high throughput dynamic network infrastructures for high performance datacentre interconnects," 2012. [Online]. Available: <http://www.ict-lightness.eu/>
- [3] S. J. B. Yoo, "Energy Efficiency in the Future Internet: The Role of Optical Packet Switching and Optical-Label Switching," *IEEE Journal of Selected Topics in Quantum Electronics*, vol. 17, no. 2, pp. 406–418, Mar. 2011. [Online]. Available: <http://ieeexplore.ieee.org/lpdocs/epic03/wrapper.htm?arnumber=5658099>
- [4] F. Ramos, E. Kehayas, J. M. Martinez, R. Clavero, J. Marti, L. Stampoulidis, D. Tsiokos, H. Avramopoulos, J. Zhang, N. Chi, P. Jeppesen, N. Yan, I. T. Monroy, a. M. J. Koonen, M. T. Hill, Y. Liu, H. J. S. Dorren, R. V. Caenegem, D. Colle, M. Pickavet, B. Ripoati, P. Holm-Nielsen, and R. Van Caenegem, "IST-LASAGNE: towards all-optical label swapping employing optical logic gates and optical flip-flops," *Journal of Lightwave Technology*, vol. 23, no. 10, pp. 2993–3011, Oct. 2005.
- [5] N. Wada, G. Cincotti, S. Yoshima, N. Kataoka, and K.-i. Kitayama, "Characterization of a Full Encoder / Decoder in the AWG Configuration for Code-Based Photonic Routers Part II : Experiments and Applications," *Journal of Lightwave Technology*, vol. 24, no. 1, pp. 113–121, 2006.
- [6] A. M. J. Koonen, N. Yan, J. J. V. Olmos, I. T. Monroy, C. Peucheret, E. V. Breusegem, and E. Zouganeli, "Label-Controlled Optical Packet Routing Technologies and Applications," *IEEE Journal of Selected Topics in Quantum Electronics*, vol. 13, no. 5, pp. 1540–1550, 2007.
- [7] N. Chi, J. Zhang, and P. Jeppesen, "All-optical subcarrier labeling based on the carrier suppression of the payload," *IEEE Photonics Technology Letters*, vol. 15, no. 5, pp. 781–783, May 2003.
- [8] I. M. White, M. S. Rogge, S. Member, K. Shrikhande, and L. G. Kazovsky, "A Summary of the HORNET Project : A Next-Generation Metropolitan Area Network," *IEEE Journal of Selected Areas In Communications*, vol. 21, no. 9, pp. 1478–1494, 2003.
- [9] J. Luo, S. D. Lucente, A. Rohit, S. Zou, K. A. Williams, H. J. S. Dorren, and N. Calabretta, "Optical Packet Switch With Distributed Control Based on InP Wavelength-Space Switch Modules," *IEEE Photonics Technology Letters*, vol. 24, no. 23, pp. 2151–2154, 2012.
- [10] S. Di Lucente, J. Luo, R. P. Centelles, A. Rohit, S. Zou, K. a. Williams, H. J. S. Dorren, and N. Calabretta, "Numerical and experimental study of a high port-density WDM optical packet switch architecture for data centers," *Optics express*, vol. 21, no. 1, pp. 263–9, Jan. 2013.
- [11] J. Luo, H. J. S. Dorren, and N. Calabretta, "Optical RF Tone In-Band Labeling for Large-Scale and Low-Latency Optical Packet Switches," *Journal of Lightwave Technology*, vol. 30, no. 16, pp. 2637–2645, 2012.

- [12] P. Seddighian, S. Member, S. Ayotte, J. B. Rosas-fernández, S. Laroche, A. Leon-garcia, L. A. Rusch, and S. Member, "Optical Packet Switching Networks With Binary Multiwavelength Labels," *Journal of Lightwave Technology*, vol. 27, no. 13, pp. 2246–2256, 2009.
- [13] N. Calabretta, P. J. Urban, D. H. Geuzebroek, E. J. Klein, H. de Waardt, and H. J. S. Dorren, "All-Optical Label Extractor/Eraser for In-Band Labels and 160-Gb/s Payload Based on Microring Resonators," *IEEE Photonics Technology Letters*, vol. 21, no. 9, pp. 560–562, May 2009.
- [14] P. De Heyn, B. Kuyken, D. Vermeulen, W. Bogaerts, and D. Van Thourhout, "High-Performance Low-Loss Silicon-on-Insulator Microring Resonators using TM-polarized Light," in *The Optical Fiber Communication Conference and Exposition (OFC) and The National Fiber Optic Engineers Conference (NFOEC) 2011*, 2011, p. OThV.
- [15] P. De Heyn, D. Vermeulen, T. Van Vaerenbergh, B. Kuyken, and D. Van Thourhout, "Ultra-high Q and finesse all-pass microring resonators on Silicon-on-Insulator using rib waveguides," in *Proceedings of the 16th European Conference on Integrated Optics and Technical Exhibition (ECIO 2012)*, 2012, pp. 1–2.
- [16] W. Bogaerts, P. De Heyn, T. Van Vaerenbergh, K. De Vos, S. Kumar Selvaraja, T. Claes, P. Dumon, P. Bienstman, D. Van Thourhout, and R. Baets, "Silicon Microring Resonators," *Laser & Photonics Reviews*, vol. 6, no. 1, pp. 47–73, 2012.
- [17] P. De Heyn, S. Verstuyft, S. Keyvaninia, A. Trita, and D. Van Thourhout, "Tunable 4-Channel Ultra-Dense WDM Demultiplexer with III-V Photodiodes Integrated on Silicon-on-Insulator," in *Asia Communications and Photonics Conference (ACP - 2012)*, 2012, pp. 8–10.
- [18] J. Luo, J. Parra-Cetina, S. Latkowski, R. Maldonado-Basilio, P. Landais, H. Dorren, and N. Calabretta, "Quantum Dash Mode-Locked Laser based Open-Loop Optical Clock Recovery for 160 Gb/s Transmission System," in *Optical Fiber Communication Conference*, 2013.

Peter De Heyn received the masters degree in photonics engineering from Ghent University and Vrije Universiteit Brussel (VUB), Belgium in 2009. He is now working towards a PhD degree in the Photonics Research Group of Ghent University and IMEC, Belgium. He was a 6 months visiting researcher at HHI Fraunhofer Institute, Berlin, Germany in 2011. His interest is optical interconnects on silicon photonics including ring resonators for filter applications, heterogeneous III-V on SOI integration, high-performance III-V and germanium photodiodes.

Jun Luo received the Ph.D. degree in optical communications from Tianjin University, Tianjin, China, in 2012. From 2010 to 2011, he was a Visiting Researcher with the COBRA Research Institute, Eindhoven University of Technology, Eindhoven, The Netherlands, where he is currently a Postdoctoral Researcher. His current research interests include optical packet switching and high-speed optical signal processing.

Stefano Di Lucente received his B.Sc. degree and M.Sc. degree in Electronic Engineering from Roma Tre University, Rome, Italy, in 2006 and 2009 respectively. He is currently working toward the Ph.D. degree in the Electro-Optical Communication group, Eindhoven University of Technology, Eindhoven, the Netherlands. His research activities are focused on optical packet switching, optical labeling techniques and optical packet switch control systems.

Harm J. S. Dorren received the M.Sc. degree in theoretical physics and Ph.D. degree from Utrecht University, Utrecht, The Netherlands, in 1991 and 1995, respectively. He joined Eindhoven University of Technology, Eindhoven, The Netherlands, in 1996, where he presently serves as a Full Professor and Scientific Director of the COBRA Research Institute. Between 1996 and 1999, he was also a part-time research associate with KPN-Research in The Netherlands. In 2002, he was a Visiting Researcher with the National Institute of Industrial Science and Technology (AIST), Tsukuba, Japan. In 2002, he received a VIDI grant and in 2006 a VICI grant by The Netherlands Organization for Scientific Research. His research interests include optical packet switching, digital and ultrafast photonics, and optical interconnects. He has authored and coauthored over 380 journal papers and conference proceedings.

Nicola Calabretta received the B.S. and M.S. degrees in telecommunications engineering from Politecnico di Torino, Turin, Italy, in 1995 and 1999, respectively, and the Ph.D. degree from the COBRA Research Institute, Eindhoven University of Technology, Eindhoven, The Netherlands, in 2004. In 1995, he visited the RAI Research Center, Turin, Italy. From 2004 to 2007, he was a Researcher with Scuola Superiore Sant'Anna University, Pisa, Italy. He is currently with the COBRA Research Institute, Eindhoven University of Technology, Eindhoven, The Netherlands. He has coauthored more than 150 papers published in international journals and conferences and holds three patents. His fields of interest are optical packet switching, semiconductor optical amplifier, all-optical wavelength conversion and regeneration, and advanced modulation formats for optical packet switching. Dr. Calabretta is currently acting as a reviewer for several IEEE, IEE, and OSA journals.

Dries Van Thourhout received the degree in physical engineering and the Ph. D. degree from Ghent University, Belgium in 1995 and 2000, respectively. From 2000 to 2002, he was with Lucent Technologies, Bell Laboratories, Crawford Hill, working on InPInGaAsP monolithically integrated devices. In 2002, he joined the Department of Information Technology (INTEC), Ghent University, continuing his work on integrated optoelectronic devices. Main interests are heterogeneous integration by wafer bonding, intrachip optical interconnect and WDM-devices.